AIP Advances

Plasma-enhanced chemical vapor deposition of graphene on copper substrates

Nicolas Woehrl, Oliver Ochedowski, Steven Gottlieb, Kosuke Shibasaki, and Stephan Schulz

Citation: AIP Advances **4**, 047128 (2014); doi: 10.1063/1.4873157
View online: http://dx.doi.org/10.1063/1.4873157
View Table of Contents: http://scitation.aip.org/content/aip/journal/adva/4/4?ver=pdfcov
Published by the AIP Publishing

AIP ADVANCES **4**, 047128 (2014)

Plasma-enhanced chemical vapor deposition of graphene on copper substrates

Nicolas Woehrl,[1,a] Oliver Ochedowski,[2] Steven Gottlieb,[2]
Kosuke Shibasaki,[3] and Stephan Schulz[1]
[1]*Faculty of Chemistry and CENIDE, University Duisburg-Essen, Carl-Benz-Straße 199, 47057 Duisburg, Germany*
[2]*Faculty of Physics and CENIDE, University Duisburg Essen, Lotharstraße 1, 47057 Duisburg, Germany*
[3]*Institute of Materials Science, Graduate School of Pure and Applied Sciences, University of Tsukuba, Tsukuba, Ibaraki 305-8573, Japan*

(Received 18 February 2014; accepted 14 April 2014; published online 22 April 2014)

A plasma enhanced vapor deposition process is used to synthesize graphene from a hydrogen/methane gas mixture on copper samples. The graphene samples were transferred onto SiO_2 substrates and characterized by Raman spectroscopic mapping and atomic force microscope topographical mapping. Analysis of the Raman bands shows that the deposited graphene is clearly SLG and that the sheets are deposited on large areas of several mm^2. The defect density in the graphene sheets is calculated using Raman measurements and the influence of the process pressure on the defect density is measured. Furthermore the origin of these defects is discussed with respect to the process parameters and hence the plasma environment. [http://dx.doi.org/10.1063/1.4873157]

I. INTRODUCTION

Graphene is a crystalline monolayer of sp^2-bonded carbon atoms arranged in a regular hexagonal pattern. This structure is the reason for the remarkable mechanical, electronic, thermal, optical and chemical properties of graphene. Optical transparence of up to 97% and electron mobility above 15000 cm^2/Vs has been reported[1] with theoretically potential limits as high as 200.000 cm^2/Vs for free-standing graphene[2] limited by the scattering of graphene's acoustic phonons. However, these values are limited by the quality of the graphene itself and the type of substrate. Due to these properties graphene is getting much attention from fundamental as well as applied science and technology. One problem that still detained this material from a broad technological implementation is the challenge to synthesize a defect-free graphene layer on larger scale, which is essential for its industrial use for example in energy applications (batteries, fuel cells) and semiconductor technology.

First methods to produce a sample of graphene was the method of mechanical exfoliation that was also used by the Nobel price laureates K. S. Novoselov and A. K. Geim using Scotch tape to pull apart the layers of a piece of highly oriented pyrolytic graphite and transfer layers from the graphite onto a SiO_2 substrate.[3] One can easily see that this method is slow and limited in size by the dimension of the highly oriented crystal, making this method expensive and not suitable for industrial applications.

One of the most promising alternatives to synthesize larger areas of high quality graphene is the use of chemical vapor deposition (CVD), in particular thermal CVD, which allows to deposit rather large areas with graphene of high quality.[4] During the low-pressure CVD process, reactive gas species (mostly H_2 and CH_4) are fed into a hot-wall reactor (temperatures at around 1000 °C)

[a]Corresponding author. Tel: +49 203 379 8126. E-Mail: nicolas.woehrl@uni-due.de

for chemical reactions. Most of these CVD processes use copper as substrates and take advantage of the catalytic influences of the copper and hydrogen.[5,6] However the high activation temperature for the catalytic reaction of methane causes significant evaporation of the substrate material even at temperatures far below the melting point of copper[5] making the process hard to control and defects in the growing graphene likely to occur. The main reason for this effect is the strong increase of copper's vapor pressure with an increasing temperature at the conditions used for the CVD of graphene.

In combination with the slow increase of temperature in a typical thermal CVD reactor (thus long process time) the process will be affected by the evaporation of a notable amount of copper. In sharp contrast, the synthesis of graphene by plasma-enhanced CVD (PECVD) can circumvent this problem by substantially shortening the process time and the prospect of lowering the substrate temperature. The reduced thermal load and the possibility to industrially scale-up the PECVD process makes it a very attractive alternative to the thermal CVD process with respect to future's graphene production.

There have been some reports of plasma-based methods to decrease the process temperature including the use of microwave plasma CVD to synthesize graphene on nickel foil,[7] surface wave plasma CVD to synthesize graphene at low temperatures in the range of 300 °C to 400 °C on large area conductive electrodes[8,9] and the plasma-assisted deposition of graphene on copper foils at temperatures down to 600 °C.[10–12] Although these works show that PECVD is a promising method for the synthesis of graphene, the resulting carbon structures often lack of quality being FLG with considerable amount of defects.[11,12] The high defect density in PECVD graphene is referred to energetic particles from the plasma interacting with the growing surface. Nevertheless there have been experiments proving that SLG of good quality can be deposited by plasma-assisted methods.[10] In this work the authors used a pulsed DC plasma reactor. According to their process, a distance must be maintained between the plasma initial stage and the deposition stage to allow the plasma to diffuse to the substrate. The deposition is therefore not taken place in the direct plasma but downstream. While that leads to a much lower defect density in the SLG it makes an additional furnace necessary to heat the sample. Another disadvantage of this method is the relatively low pressure that the deposition is taking place (0.5 torr).

In this work we present the synthesis of SLG graphene on copper with a direct microwave PECVD system on large areas which is beneficial in two ways: Firstly, due to the fact that the copper substrate is positioned directly in the plasma, the substrate is heated by the plasma and no additional furnace is necessary. Secondly the special construction of the plasma source allows the deposition at a wide range of different process parameters especially at higher pressures. Both, the direct plasma heating and the faster and less cost intensive CVD process due to the higher pressure make this method attractive for potential future industrial applications. Nevertheless as previously shown the direct plasma treatment can course defects in the SLG. In this work the effect of the process parameters on the defect density is shown.

II. EXPERIMENTAL

Graphene films were deposited with a 2.45 GHz IPLAS *CYRANNUS*® I-6″ plasma source. The maximum power input is limited to 5 kW by the microwave power generator. The functional principle of this microwave plasma source is based on a resonator with annular slot antennas.[13] This special setup allows the use of plasma from low pressure (10^{-2} mbar) to atmospheric pressure (1 bar) and above.

The reaction chamber is a cylindrical shaped quartz tube with a diameter of 140 mm and a height of 140 mm. The process gas is fed into the process chamber by a gas shower in the top flange and a molybdenum substrate holder of 100 mm diameter is mounted on the bottom flange (Fig. 1). The substrate is placed right below the plasma.

Graphene films were deposited on 50-μm-thick copper foil (Puratronic 99.9999%, item No.: 42972, Alfa Aesar GmbH & Co KG, Karlsruhe, Germany) similar to those described elsewhere.[5] The copper surface was cleaned by a hydrogen plasma treatment before starting the graphene deposition.

The PECVD process uses hydrogen and methane as reaction gases as is typically done in thermal CVD process. The chemical fundamentals of the synthesis are based on a physisorption process of

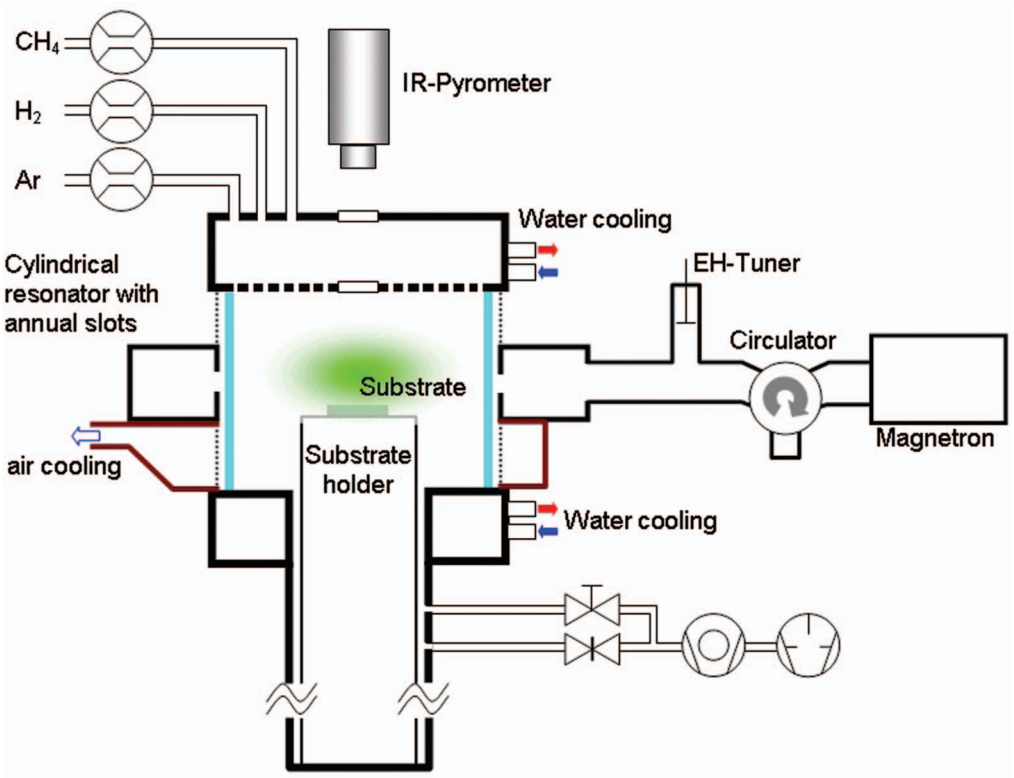

FIG. 1. Schematic diagram of the microwave plasma source and the substrate holder.

TABLE I. Process Parameters for MW-PECVD of graphene on copper foil.

		Cleaning Process			Synthesis		
Pressure	Power	Time	H_2-flow	CH_4-flow	Time	H_2-flow	CH_4-flow
20–80 mbar	1 kW	20 min	200 sccm	–	10 min	200 sccm	25 sccm

hydrogen and a consecutive chemisorption process of methane.[14] Physically adsorbed H_2 molecules decompose due to the high temperature on the copper surface. Consecutively chemisorption of methane molecules results in carbon species bonded to the top layered copper atoms, which become successively dehydrogenized and eventually building the graphene's honeycomb pattern. Due to the catalytic influence of copper and the minor solubility of carbon in copper, this leads to the growth of monolayer graphene. The graphene growth process is self-limiting and therefore basically stops after the growth of a monolayer.[5]

Graphene deposition. After placing the copper foil in the center of the reaction chamber the reactor was evacuated to $1 \cdot 10^{-5}$ mbar. Hydrogen (200 sccm) was introduced in the chamber and a plasma was ignited at a pressure of 5 mbar with a microwave power of 1 kW. Plasma cleaning was performed for 20 minutes to clean the substrate from all remaining organic contaminations and for chemical reduction of the surface. During that time the pressure was raised. Pressure was varied between 20 and 80 mbar for the different experiments. A suitable substrate temperature for the deposition process was reached by direct plasma heating and was measured with an optical pyrometer to be $900 \pm 20\,^{\circ}C$. The synthesis of graphene starts with the introduction of 25 sccm methane in the process chamber and was performed for ten minutes with the methane-hydrogen plasma at constant pressure and substrate temperature. After that time the reactor was immediately evacuated to inhibit the etching influence of hydrogen on carbon structures at high temperatures.[15] The process parameters can be found in Table I.

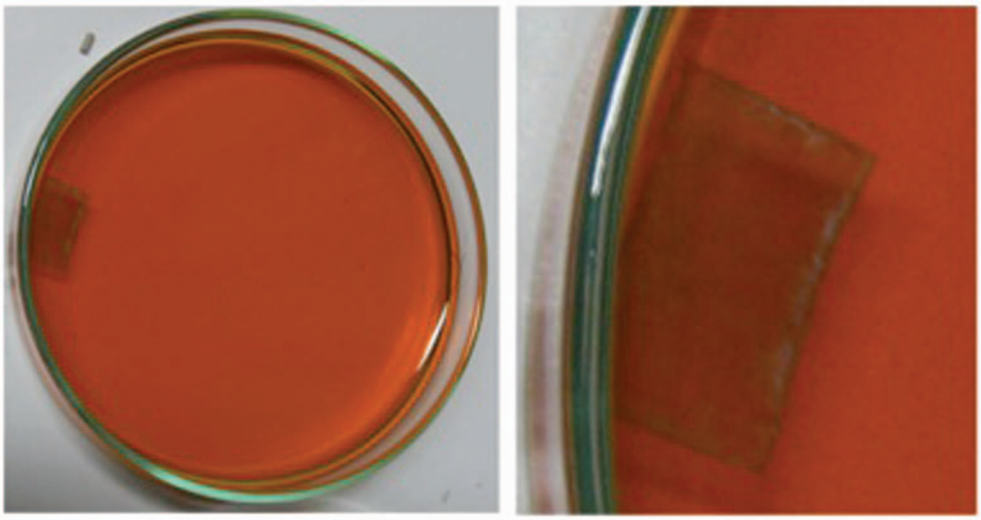

FIG. 2. Graphene on PMMA swimming on surface of $FeCl_3$ solution.

Raman spectroscopy is used for the characterization of graphene, which is a popular non-destructive analytical tool used to characterize the structure of the graphitic materials.[16] Raman spectroscopy is also suitable to determine the number of graphene layers, the disorder and the doping of the graphene.[17,18] The Raman spectra in this paper were measures with a Renishaw inVia REFLEX Raman spectrometer with a 532 nm (2.34 eV) and a 633 nm (1.96 eV) laser.

The Raman spectrum of graphene has a few prominent features. The G-band at around 1580 cm^{-1} arises from the E_{2g} in-plane vibration of the sp^2 carbon atoms. Two additional features, the D-band which is assigned to the A_{1g} breathing mode at the Brillouin Zone boundary K and the D′-band appear at around 1330 and 1620 cm^{-1}, respectively, when point defects are introduced in the graphene layer as demonstrated in a controlled manner by ion implantation.[19] Therefore I_D/I_G intensity ratio can be used to quantify disorder in a graphene monolayer by determining the average distance between defects L_D.[20] Moreover, for large disorder also the full width at half-maximum (FWHM) of the D and the G-band is even a better measure for structural disorder.[21]

The D+D′ band (around 2920 cm^{-1}) is the combination of phonons with different momenta around K and Γ and therefore also is a measure for defects.

The 2D band is the second order of the D band.[22,23] Since the 2D band originates from the momentum conservation by two phonons with opposite wave vectors, no defects are required for its activation. The shape of the 2D band is of special interest because it provides information about the number of graphene layers in the material. In the case of single-layer graphene, the 2D band is fitted by a single narrow Lorentzian function. A FWHM of 33 cm^{-1} (measured with 532 nm) for the 2D band is typically assigned to SLG,[37] while for few-layer samples the 2D feature is becoming significantly broader and asymmetric. The bilayer has a much broader and up-shifted 2D band with respect to single-layer graphene due to its special electronic structure, consisting of two conduction bands and two valence bands.[16,17,24] Additionally, the intensity of the G band increases with increasing layer thickness, which allows further estimation of the layer thickness.[25,26]

Ex situ atomic force microscopy (AFM, Veeco Dimension 3100) is used to determine the film thickness and surface morphology after the transfer process.

III. RESULTS

The PECVD process was used to deposit graphene on a 20 × 10 mm copper sample. After the deposition $FeCl_3$ was used to dissolve the copper in order to remove the graphene from the substrate. The photography shown in Fig. 2 shows the graphene film on PMMA swimming in $FeCl_3$ solution. It is shown that a carbon film was deposited on the whole area of the copper substrate. Not only that

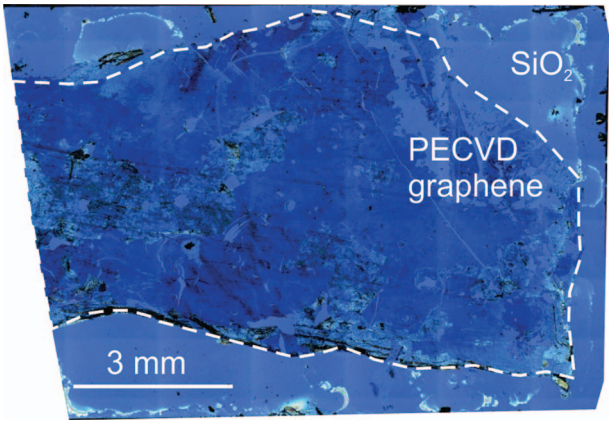

FIG. 3. PECVD graphene transferred onto a 90 nm SiO_2 substrate using PMMA.

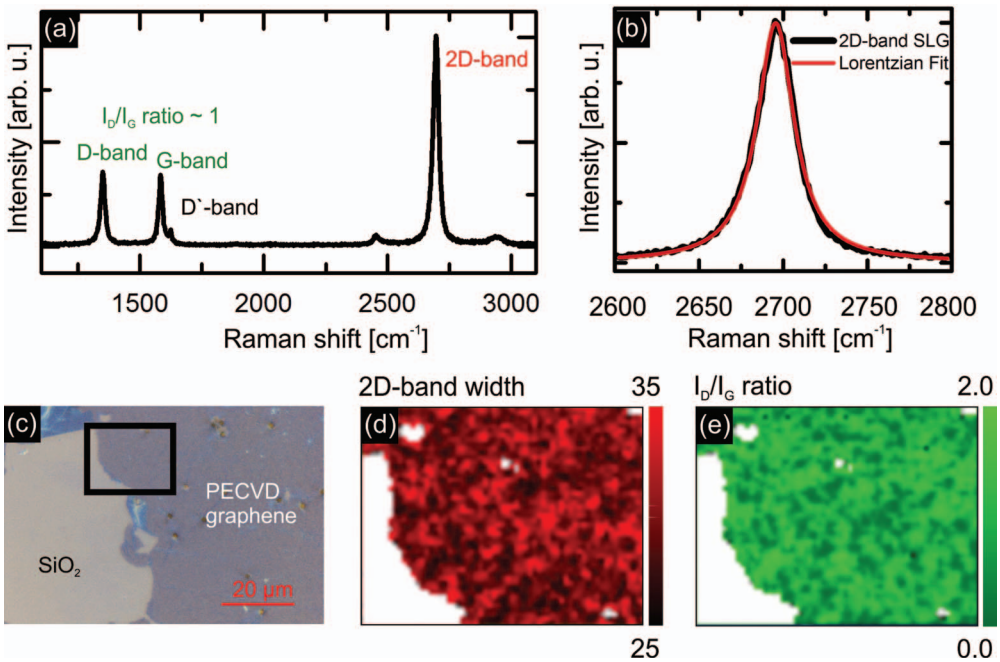

FIG. 4. a) μ-Raman spectrum taken in the center of the black box marked in (c) b) Enlarged 2D band region with Lorentzian curve fitting indicating SLG c) Optical microscope image (100× magnification) of a transferred PECVD graphene sheet on SiO_2 d) Raman map of 2D band width distribution e) Raman map of the I_D/I_G ratio.

the film has no visible holes, it is stable enough to be transferred onto a 90 nm SiO_2 substrate using PMMA. Almost the whole sample is covered by graphene which can be deduced by the optical contrast in Fig. 3. Though the transfer visibly caused damage in the graphene sheet, large areas of several mm^2 where the graphene sheet is intact can be found.

Fig. 4(a) shows a μ-Raman spectrum that was taken in the center of the black box marked in optical microscope image (Fig. 4(c)). Prominent bands in the Raman spectrum of graphene are denoted and show the typical features of graphene layers. Additionally the 2D band was fitted with a single Lorentzian shaped curve at various positions on the sample as shown in Fig. 4(b). The symmetric shape and narrow width of the 2D band (26.8 cm^{-1}) suggest that the synthesized graphene is in fact a single layer (SLG). In case of a possible AB-stack sequence of bilayer graphene a slight shoulder on its left side would be visible, which is not the case for our samples[27] at any point measured.

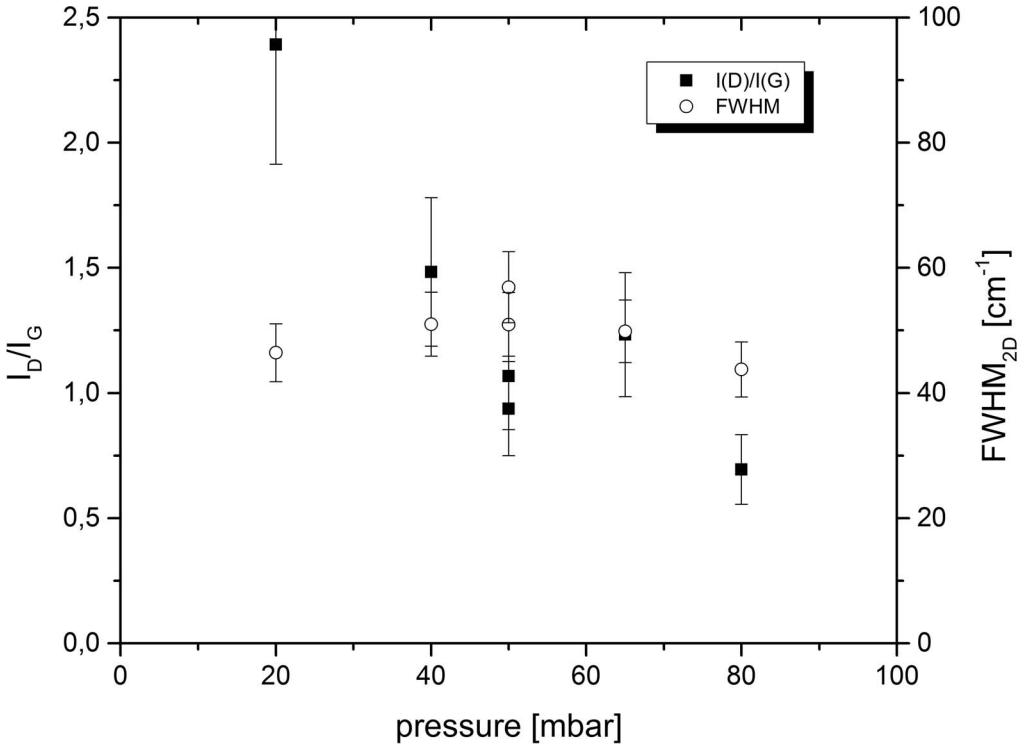

FIG. 5. I_D/I_G ratio and FWHM of the 2D peak as a function of the process pressure.

The optical microscope image (100× magnification) of the transferred PECVD graphene sheet is shown in Fig. 4(c). A large hole and Fe residues caused by the transfer process can be observed on the left side of the area.

To investigate the quality and proof the homogeneity of the synthesized graphene films Raman mapping ($\lambda = 532$ nm, $P < 2.0$ mW, step size 0.5 μm, area $= 31.5 \times 27.5$ μm^2) has been performed inside the black box in Fig. 4(c). The Raman map in Fig. 4(d) shows the 2D band FWHM distribution that ranges from 25 to 35 nm over the given area, which is a clear indication for single layer graphene.[37] The variation is most likely caused by local defect accumulation as well as ripples in the graphene sheet. Additionally a Raman map of the I_D/I_G ratio was measured, revealing an average ratio of 0.9 +/− 1.4. The existence of strong D-band is indicating a relatively high amount of defects in the graphene film. Additionally, as mentioned above, the D + D′ band at 2921.5 cm^{-1} and D′ at 1619.9 cm^{-1} are giving additional hints that the deposited graphene is defective. Comparing these results with the works of Cançado *et al.*[21] we can estimate the distance between point like defects L_D in the graphene monolayer. The I_D/I_G ratios measured here are indicating an average distance L_D between defects of about 10 nm. Additionally the rather sharp G and D bands (with FWHM between 15 and 22 cm^{-1} and between 19 and 26 cm^{-1}, respectively) could support this interpretation even though these values can also be influenced by stress and doping of the material, which can't be excluded in this work.

Since one explanation for the high defect density in PECVD graphene is energetic particles from the plasma interacting with the growth surface, the influence of process- (hence plasma-) parameters on the quality of the graphene was investigated by variation of process pressure. Fig. 5 shows the I_D/I_G ratio and the FWHM of the 2D band as a function of the pressure during deposition. One can see, that the I_D/I_G ratio decreases from 2.5 for 20 mbar to 0.75 at 80 mbar. At the same time the FWHM of the 2D peak stays nearly constant at 50 +/− 10 cm^{-1}. Comparing these measurement with the measurements done in[21] we can estimate that the distance between defects is reduced from around 5 nm to around 15 nm by increasing the pressure from 20 to 80 mbar.

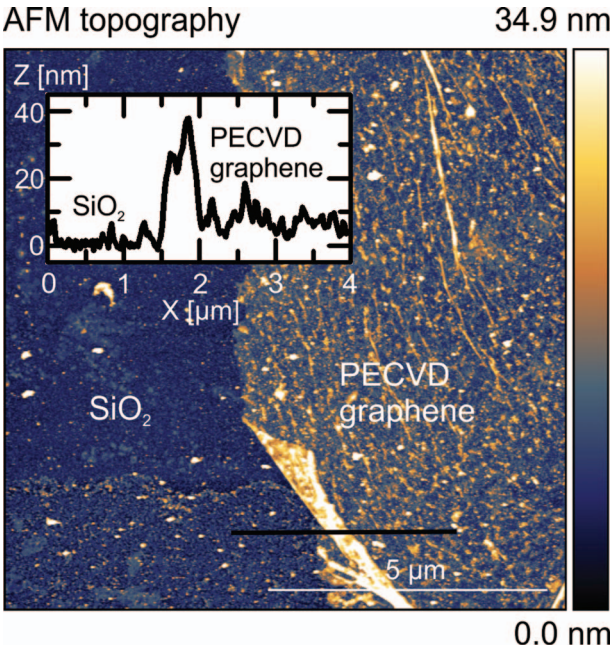

FIG. 6. AFM topography (tapping mode) image.

AFM topography measurements in tapping mode (Fig. 6) were performed of the area located inside the black box of Fig. 4(c). The topography shows that the graphene as well as SiO_2 is decorated with contamination due to the transfer process. The line profile (averaged over 5 lines) shows a height of 1.4 nm and a large roughness on the graphene flake of 9.0 nm compared to the 3.8 nm of the contaminated SiO_2 substrate. As pristine graphene normally shows a lower roughness as its substrate, defects, ripples, wrinkles and folding observed parallel to the graphene edge are the most likely causes.

IV. DISCUSSION

Raman mapping confirmed the SLG nature of the deposited carbon film over most of the substrate surface. This result suggests that the process developed is able to produce rather large areas of graphene - only limited by the microwave plasma radius. Thus the given setup at present allows the deposition on areas of up to 100 mm diameter, allowing the processing of standard 4-inch silicon wafer sized substrates.

Raman measurements proofed the homogenous structure and quality, however the synthesized graphene films show a relatively high density of defects. It was previously reported that ion bombardment,[21] electron bombardment[28] and EUV radiation[29] lead to similar evolution of the Raman spectra. Furthermore, graphene hydrogenation occurs due to presence of hydrogen species in the plasma.[30,15] Based on prior studies the dominant species in a weakly ionized hydrogen discharge at the given process parameters (ionization rate below 0.1%) are hydrogen radicals (1%) and H_3^+ ions (0.1%).[31] Since all these particles are created in the plasma the surface will interact with all these species generating vacancies and vacancy clusters in the graphene layer.

In fact, introduction of surface defects in combination with a mild hydrogen plasma etching process could be responsible for the observation that nearly the whole substrate surface is deposited with only a SLG. The rate of hydrogenation of graphite along the lateral (in-plane) direction is higher compared to the vertical direction due to the anisotropic crystal structure. Thus, the formation of a second layer of graphene will be suppressed by a simultaneous etching process. The introduction of defects in the layer will even increase the speed of etching due to the creation of dangling bonds and hydrogenation sites at the surface. Similar etching effects of remote hydrogen plasmas were

previously reported.[32] However, in contrast to these studies, we are not observing high monolayer selectivity but in fact do not observe any etching of the monolayer at all. We believe that this is due to the fundamental differences in the studies given that we use a carbon source gas in addition to hydrogen while in[32] hydrogen alone was used to study the etching. Hence we believe that two competing mechanisms occur in our process with a simultaneous etching of graphene and the deposition of carbon on the surface at the same time.

Since electric[33] and thermal conductivity[34] is strongly decreased by the defects on the one hand and chemical reactivity is enhanced due to dangling bonds associated with these defects on the other[35] the influence of process parameters on the defect density were investigated. It was shown that the defect density is lower for higher pressures. There are two possible explanations for this effect. Firstly the plasma ball is slightly shrinking with higher pressure. Since the position of the substrate under the plasma and the position of the plasma ball center is fixed we effectively observe a bigger distance between the plasma ball and the substrate at higher pressures. Since the mean free path of particles from the plasma is roughly $1.36 \cdot 10^{-3}$ mm at a pressure of 50 mbar the change of the plasma size will greatly influence the number of energetic particles from the plasma interacting with the surface.

Secondly the change in process pressure can also lead to changes in the plasma chemistry. Future works will include plasma monitoring by optical emission spectroscopy and mass spectroscopy to investigate this possible influence.

In our experiments we were not able to synthesize graphene at lower temperatures than 800 °C. This is in good agreement with the temperature dependence of the etching rate found in[32] where the highest reaction rates occurred between 500 and 600 °C and decreased for higher temperatures. In our experiments the etching effect is the dominating process at lower temperatures and thus suppressing any graphene synthesis on the surface. At higher substrate temperatures however etching rate is decreased resulting in the formation of a graphene films.

AFM measurements show a high surface roughness of the graphene sheet after transferring it to the SiO_2 substrate. The AFM image shows topographical lines parallel to the graphene edge suggesting that wrinkles of the graphene layer are observed here. Such wrinkle features are frequently seen in CVD-grown samples. These features are measured to have a width between few tens of nanometers with length of several microns in our samples. The distance between single wrinkles range from tens of nanometer up to several hundred nanometers. Although graphene has a very high in-plane Young's modulus it can easily be warped in the out-of-plane direction, resulting in wrinkles just as measured in this work. While the folding is introducing strain energy to the system, the total energy can be lowered by plane-plane interactions after folding. The wrinkling of the SLG can also be the reason for the variation in I_D/I_G ratio and $FWHM_{2D}$ measured by Raman mapping. At this point it is unclear when the wrinkling of the graphene occurs. It could either happen during the synthesis, the transfer process or later on the SiO_2 substrate. Since wrinkled graphene exhibit interesting new and distinct properties the evolution of the wrinkling is important from a fundamental point of view, as well as technological relevant[36] and will be addressed in future work.

V. SUMMARY

A fast, versatile and reproducible PECVD method for the synthesis of SLG on large areas at high pressures is presented. It was shown that SLG sheets of several mm^2 were deposited on copper substrates and successfully transferred on SiO_2 surfaces. The graphene layers are of good quality although containing some defects. These defects can be beneficial when used as chemical sensors or for systematic doping of the graphene in future work. Hence the control of the defect density and the dependence from the process parameters (namely pressure) was investigated and a correlation between the pressure and the defect density was found. Future investigations should help to further determine the origin of these defects by correlating the plasma properties with the resulting SLG properties. By that it is possible to tailor the properties of the SLG with respect to a given application.

The special construction of the plasma source used in this work allows the deposition at a wide range of different process parameters. In the future the process can therefore be scaled up to

even higher pressures allowing fast and inexpensive processes and thus the implementation of this technology on an industrial level.

[1] S. J. Wang, Y. Geng, Q. B. Zheng, and J. K. Kim, Carbon **8**, 1815 (2010).
[2] A. Akturk and N. Goldsman, J. Appl. Phys. **103**, 053702 (2008).
[3] K. S. Novoselov, A. K. Geim, S. V. Morozov, D. Jiang, Y. Zhang, S. V. Dubonos, I. V. Grigorieva, and A. A. Firsov, Science **306**, 666 (2004).
[4] A. Reina, X. Jia, J. Ho, D. Nezich, H. Son, V. Bulovic, and M. S. Dresselhaus, J. Kong, Nano Letters **9**, 30 (2009).
[5] X. Li, W. Cai, J. An, S. Kim, J. Nah, D. Yang, R. Piner, A. Velamakanni, I. Jung, E. Tutuc, S. K. Banerjee, L. Colombo, and R. S. Ruoff, Science **324**, 1312 (2009).
[6] I. Vlassiouk, M. Regmi, P. Fulvio, S. Dai, P. Datskos, G. Eres, and S. Smirnov, ACS Nano. **5**, 6069 (2011).
[7] Y. Kim, W. Song, S. Y. Lee, C. Jeon, W. Jung, M. Kim, and C. Y. Park, Appl. Phys. Lett. **8**, 263106 (2011).
[8] J. Kim, M. Ishihara, Y. Koga, K. Tsugawa, M. Hasegawa, and S. Iijima, Appl. Phys. Lett. **8**, 091502 (2011).
[9] G. Kalita, K. Wakita, and M. Umeno, RSC Adv. **8**, 2815 (2012).
[10] S. H. Chan, S. H. Chen, W. T. Lin, M. C. Li, Y. C. Lin, and C. C. Kuo, Nanoscale Res. Lett. **8**, 285 (2013).
[11] A. Malesevic, R. Vitchev, K. Schouteden, A. Volodin, L. Zhang, G. van Tendeloo, A. Vanhulsel, and C. Van Haesendonck, Nanotechnology **19**, 305604 (2008).
[12] J. H. Kim, E. J. D. Castro, Y. G. Hwang, and C. H. Lee, J. Korean Phys. Soc. **58**(1), 53 (2011).
[13] CYRANNUS® I. European Patent 0872164, USA Patent 6198224, 2001.
[14] W. Zhang, P. Wu, Z. Li, and J. Yang, J. Phys. Chem. **115**, 17782 (2011).
[15] Y. Zhang, Z. Li, P. Kim, L. Zhang, and C. Zhou, ACS Nano **6**, 126 (2012).
[16] L. Malard, M. Pimenta, G. Dresselhaus, and M. Dresselhaus, Phys. Rep. **473**, 51 (2009).
[17] A. C. Ferrari, J. C. Meyer, V. Scardaci, C. Casiraghi, M. Lazzeri, F. Mauri, S. Piscanec, D. Jiang, K. S. Novoselov, S. Roth, and A. K. Geim, Phys. Rev. Lett. **97**, 187401 (2006).
[18] C. Casiraghi, S. Pisana, K. Novoselov, A. Geim, and A. Ferrari, Appl. Phys. Lett. **91**, 233108 (2007).
[19] M. S. Dresselhaus, A. Jorio, M. Hofmann, G. Dresselhaus, and R. Saito, Nano Lett. **10**, 751 (2010).
[20] M. M. Lucchese, F. Stavale, E. H. Martins Ferreira, C. Vilani, M. V. O. Moutinho, R. B. Capaz, C. A. Achete, and A. Jorio, Carbon **48**, 1592 (2010).
[21] L. G. Cançado, A. Jorio, E. H. Martins Ferreira, F. Stavale, C. A. Achete, R. B. Capaz, M. V. O. Moutinho, A. Lombardo, T. S. Kulmala, and A. C. Ferrari, Nano Lett. **11**, 3190 (2011).
[22] F. Tuinstra and J. Koenig, J. Chem. Phys. **53**, 1126 (1970).
[23] A. Gupta, G. Chen, P. Joshi, S. Tadigadapa, and P. Eklund, Nano Lett. **6**, 2667 (2006).
[24] A. Jorio, M. Dresselhaus, R. Saito, G. Dresselhaus, *Raman Spectroscopy in Graphene Related Systems*, 1st ed. (Wiley, Weinheim, 2010).
[25] Y. Y. Wang, Z. H. Ni, Z. X. Shen, H. M. Wang, and Y. H. Wu, Appl. Phys. Lett. **92**, 043121 (2008).
[26] Z. Ni, Y. Wang, T. Yu, and Z. Shen, Nano Res. **4**, 273 (2010).
[27] A. C. Ferrari, Science direct, Solid State Communications **143**, 47 (2007).
[28] D. Teweldebrhan and A. A. Balandin, Appl. Phys. Lett. **94**, 013101 (2009).
[29] A. Gao, P. J. Rizo, E. Zoethout, L. Scaccabarozzi, C. J. Lee, V. Banine, and F. Bijkerk, J. Appl. Phys. **114**, 044313 (2013).
[30] D. C. Elias, R. R. Nair, T. M. G. Mohiuddin, S. V. Morozov, P. Blake, M. P. Halsall, A. C. Ferrari, D. W. Boukhvalov, M. I. Katsnelson, A. K. Geim, and K. S. Novoselov, Science **323**, 610 (2009).
[31] S. Nunomura and M. Kondo, J. Appl. Phys. **102**, 093306 (2007).
[32] G. Diankov, M. Neumann, and D. Goldhaber-Gordon, ACS Nano **7**, 1324 (2013).
[33] A. Cortijo and M. Vozmediano, Nuclear Physics B **763**, 293 (2007).
[34] F. Hao, D. Fang, and Z. Xu, Appl. Phys. Lett. **99**, 041901 (2011).
[35] D. Boukhvalov and M. Katsnelson, Nano letters **8**, 4373 (2008).
[36] K. Kim, Z. Lee, B. D. Malone, K. T. Chan, B. Alemán, W. Regan, W. Gannett, M. F. Crommie, M. L. Cohen, and A. Zettl, Phys. Rev. B **83**, 245433 (2011).
[37] C. Stampfer, F. Molitor, D. Graf, K. Ensslin, A. Jungen, C. Hierold, and L. Wirtz, Appl. Phys. Lett. **91**, 241907 (2007).